

Some Aspects of Helicopter Flight Dynamics in Steady Turns

Giorgio Guglieri*

Turin Polytechnic Institute, 10129 Turin, Italy

and

Roberto Celi†

University of Maryland, College Park, Maryland 20742

Results are presented of a theoretical study of the flight dynamics and handling qualities of hingeless rotor helicopters in turning flight. Frequency responses in pitch, roll, and heave are evaluated for various advance ratios, turn rates, and turn directions; comparisons are made with criteria of the ADS-33 handling qualities specifications. The results show that couplings between lateral and longitudinal dynamics are present in turning flight. Flight speed, load factor, and direction of turn affect frequency and damping of both poles and zeros. Zeros that are stable in straight flight can become lowly damped or nonminimum phase and cause a deterioration of handling qualities. This may also cause flight control systems designed for straight flight to perform poorly in some turning flight conditions. The bandwidth criteria of the ADS-33 specifications do not explicitly address maneuvering flight conditions. Therefore, there remains an open question of whether the degradations of handling qualities identified in this study are real (possibly through mechanisms other than those intended in the original formulation of the specification) or a mathematical artifact.

Nomenclature

n_T	= load factor
ζ	= damping ratio
θ	= pitch attitude, rad
θ_{1c}	= lateral cyclic, rad
θ_{1s}	= longitudinal cyclic, rad
μ	= advance ratio
τ_p	= phase delay, s
ϕ	= roll attitude, rad
ω_{BW}	= bandwidth, rad/s
ω_n	= undamped natural frequency, rad/s

Introduction

THE formulation and application of helicopter handling qualities criteria have been the focus of extensive research, especially in the last decade. Much of this work has been prompted by the development and validation of the U.S. Army ADS-33 handling qualities specifications.¹ A detailed review of these activities is beyond the scope of the present paper; a thorough discussion of the fundamental issues associated with the quantification of helicopter handling qualities characteristics and an extensive list of pertinent references can be found in a recent textbook by Padfield.²

This paper addresses one specific flight condition, namely, a coordinated steady turn. ADS-33 does not include quantitative handling qualities criteria that explicitly address coordinated turns, except for limits on the roll-to-sideslip coupling. In particular, no mention of the flight regime is made in the requirements on the short-term response to control inputs for small-amplitude attitude changes. These requirements were formulated based on supporting data that did not include real or simulated turning flight conditions.

The flight dynamics of helicopters in turns has not been studied extensively. The first systematic studies are due to Chen and Jeske,³ Chen et al.,⁴ and Chen.⁵ References 3 and 4 established procedures for the calculation of the trim state in coordinated and uncoordinated, steady, helical turns. Reference 5 was a systematic investigation of the flight dynamics of various types of rotorcraft in steep, high-g

turns. Among the conclusions of the study were that 1) strong couplings between longitudinal and lateral directional dynamics exist in high-g turns; 2) the direction of turn has a significant influence on the flight dynamic characteristics; and 3) the characteristics of a hingeless rotor helicopter equipped with a stability and control augmentation system (SCAS), otherwise satisfactory for 1-g flight, can become seriously degraded in steep turning flight. The short-period longitudinal dynamics of the Westland Puma helicopter was studied by Houston.⁶ The study included a systematic analytic evaluation of stability and control derivatives at various turn rates and an assessment of the adequacy of various reduced-order models. One of the conclusions was that the conventional short-period approximation is inadequate, primarily because of the strong coupling between longitudinal and lateral directional dynamics in banked turns. The trim formulation of Ref. 3 was extended in Ref. 7 to include the steady-state response of flexible rotor blades and was used in an analysis of the aeroelastic stability of hingeless rotors in steady turns. The aeroelastic analysis did not include the dynamic coupling between rotor and fuselage, which was later added by Spence and Celi.⁸ Both Refs. 7 and 8 address turning flight conditions, but the focus was on aeroelasticity and aeromechanics, rather than flight dynamics and handling qualities.

The general objective of this paper is to present the results of a theoretical study of the flight dynamics and handling qualities of a hingeless rotor helicopter in a coordinated steady turn. Two specific objectives, not addressed by previous research, are to 1) study the frequency response of the helicopter to pilot inputs in pitch, roll, and heave, for different advance ratios, load factors, and directions of turn and 2) study the handling qualities characteristics in pitch and roll of the helicopter in turning flight, using the methodology of the ADS-33 handling qualities specifications for the short-term response to control inputs and small-amplitude attitude changes.

Mathematical Model

Formulation

The mathematical model of the helicopter used in this study is a nonlinear blade element model that includes fuselage, rotor, main rotor inflow, and propulsion system dynamics. The six-degree-of-freedom rigid-body motion of the aircraft is modeled using nonlinear Euler equations. Linear aerodynamics is assumed for fuselage and empennage.

The blades are assumed to be rigid, with offset hinges and root springs selected so as to achieve fundamental natural frequencies in flap and lag of 1.125/rev and 0.7/rev, respectively. Flap and lag dynamics of each blade are modeled. The main rotor has four blades.

Received March 19, 1997; revision received Oct. 21, 1997; accepted for publication Oct. 24, 1997. Copyright © 1997 by Giorgio Guglieri and Roberto Celi. Published by the American Institute of Aeronautics and Astronautics, Inc., with permission.

*Assistant Professor, Dipartimento di Ingegneria Aeronautica e Spaziale, Corso Duca degli Abruzzi 24. Member AIAA.

†Associate Professor, Department of Aerospace Engineering, Center for Rotorcraft Education and Research. Member AIAA.

Unsteady aerodynamic effects are modeled using the Pitt-Peters dynamic inflow model.⁹ The propulsion system model is a slightly modified version of that used by Chen.¹⁰

The coupled system of rotor, fuselage, inflow, and propulsion system equations of motion is written in first-order form. The state vector has a total of 32 elements: flap and lag displacements and rates for each of the 4 blades (16 states); 9 rigid-body velocities, rates, and attitudes; 3 inflow states; and 2 propulsion system angles and angular velocities.

Solution Methods

The trim procedure is the same as in Refs. 3 and 7. Thus, the rotor equations of motion are transformed into a system of nonlinear algebraic equations using a Galerkin method. The algebraic equations enforcing force and moment equilibrium, and additional kinematic equations that must be satisfied in a turn, are added to the rotor equations, and the combined system is solved simultaneously. The solution yields the harmonics of a Fourier series expansion of the rotor degrees of freedom, the pitch control settings, trim attitudes and rates of the entire helicopter, and main and tail rotor inflow. The propulsion system is not included in the trim process. This implies two assumptions: that the engine can generate a sufficient torque in any flight condition and that the small fluctuations of rotor speed associated with the lag dynamics of the rotor in trim do not affect the engine torque.

Small perturbation equations of motion are obtained by numerical linearization of the nonlinear equations about a trimmed condition. Because the equations of motion of the blades are formulated and solved in a rotating coordinate system, a multiblade coordinate transformation is used to transform the linearized system entirely into nonrotating coordinate systems. The transformation removes most of the periodicity of the equations; the residual periodic terms are averaged over one rotor revolution, so that the final linearized system is time invariant. This system is used to calculate frequency responses, poles, and zeros.

Results

The basic characteristics of the hingeless helicopter configuration used are presented in Table 1. This configuration is representative of a typical medium-size helicopter, but it is not meant to reflect any particular existing aircraft. A multidimensional matrix of test cases was studied, consisting of variations of the following parameters:

- 1) Advance ratios μ are equal to 0.1 and 0.2.
- 2) Load factors n_T are equal to 1 (straight flight), 1.125, 1.25, 1.375, and 1.5. The load factor was defined as³

$$n_T = \sqrt{1 + (\dot{\psi} V/g)^2} \tag{1}$$

where $\dot{\psi}$ is the turn rate, V is the velocity along the trajectory, and g is the acceleration due to gravity. Turn rates, advance ratios, and load factors are shown in Fig. 1.

- 3) Directions of turn are right handed, or clockwise when viewed from above ($\dot{\psi} < 0$), and left handed ($\dot{\psi} > 0$).

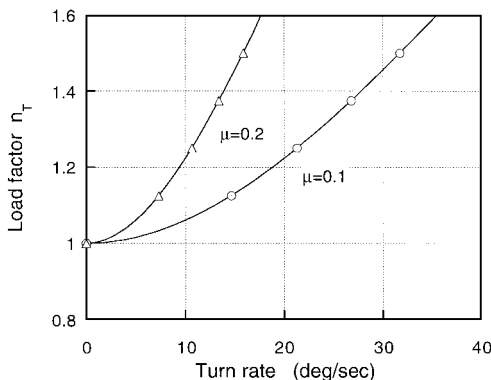


Fig. 1 Load factor n_T as a function of advance ratio and turn rate; the symbols indicate the values used in the study.

Table 1 Helicopter configuration used

Rotor speed	22 rad/s
Rotor disk radius R	9 m
Blade mean aerodynamic chord	0.6 m
Rotor hinge offset e	1.125 m /12.5%
I_{XX}	10,000 kgm ²
I_{YY}	54,000 kgm ²
I_{ZZ}	47,000 kgm ²
I_{ZX}	2,500 kgm ²
Mass	9,075 kg
Rotor solidity σ	0.0849
C_T/σ (hover)	0.0857
Lock number γ	7.78916
Blade mass per unit length	16 kg/m
Number of blades (main rotor)	4
Blade twist	0 rad
Horizontal distance between c.g. and rotor	0 m
Vertical distance between c.g. and rotor	2.25 m
Horizontal tail surface	4.15 m ²
Horizontal distance between c.g. and horizontal tail	9.9 m
Vertical distance between c.g. and horizontal tail	-0.45 m
Vertical tail surface	3.04 m ²
Horizontal distance between c.g. and vertical tail	10.66 m
Vertical distance between c.g. and vertical tail	0.91 m
Horizontal distance between c.g. and tail rotor	11.1 m
Vertical distance between c.g. and tail rotor	1.8 m
Number of blades (tail rotor)	3
Tail rotor radius	1.95 m
Tail rotor speed	100 rad/s
Tail rotor mean aerodynamic chord	0.3 m
Fundamental flap frequency	1.125/rev
Fundamental lag frequency	0.7/rev
Shaft stiffness	541,065 Nm/rad
Engine-drive train inertia I_{eq}	1,673 kgm ²
Hub inertia I_{hub}	164 kgm ²
Damping of propulsion system	0 Nm s/rad
Pitch feedback to longitudinal cyclic K_θ	-0.2

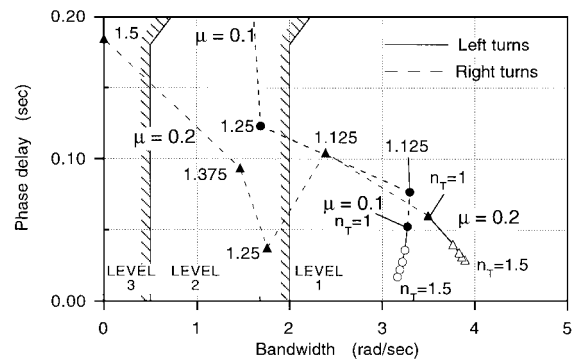


Fig. 2 Effect of load factor n_T , advance ratio μ , and direction of turn on pitch bandwidth and phase delay.

Pitch Dynamics

Significant changes occur in turning flight conditions in both the magnitude and the phase of the on-axis pitch response, especially in the region between 1 and 8 rad/s that plays an important role in defining the handling qualities of the aircraft. Figure 2 shows bandwidth and phase delay in pitch, calculated according to the criteria of ADS-33D.¹ The handling qualities level boundaries are those specified by paragraph 3.4.1.1 of ADS-33D for the target acquisition and tracking mission task element. (However, it should be remembered that the specifications do not explicitly cover turning flight conditions.) Figure 2 indicates that the load factor has a profound influence on the handling qualities of this helicopter configuration. In straight flight and gentle turns, the helicopter has level 1 handling qualities at both $\mu = 0.1$ and 0.2 and is phase limited, that is, the phase bandwidth is lower than the gain bandwidth, and the overall bandwidth is taken to be the former.¹ For $\mu = 0.1$, the phase and the gain bandwidths are almost the same for $n_T = 1.125$; the helicopter becomes gain limited in pitch for higher load factors. This is accompanied by a drastic degradation of the handling qualities:

Downloaded by Giorgio Guglielmi on November 2, 2012 | http://arc.aiaa.org | DOI: 10.2514/2.4270

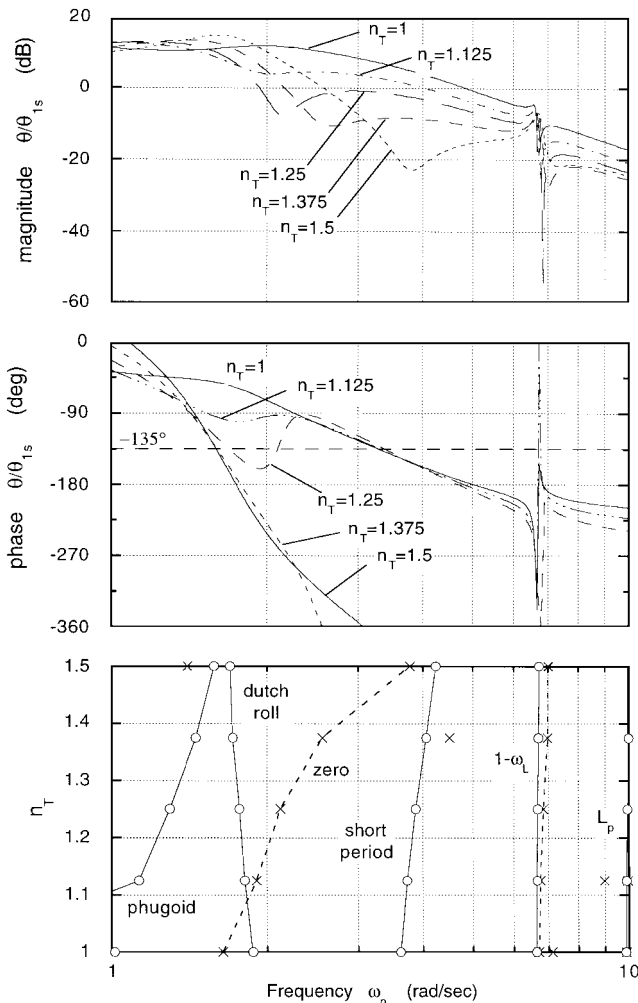


Fig. 3 Effect of load factor n_T on pitch frequency response and on poles and zeros; right-handed turns at $\mu = 0.1$.

for $n_T = 1.250$ the helicopter crosses the level 2 boundary; for $n_T = 1.375$ and 1.5 sudden dramatic decreases of the bandwidth and increases of the phase delay place the representative points well inside the level 3 region. Similar trends can be seen for right-handed turns at $\mu = 0.2$. The bandwidth decreases from $\omega_{BW} = 3.5$ rad/s for $n_T = 1$ to $\omega_{BW} = 1.4$ for $n_T = 1.375$. For $n_T = 1.5$, a bandwidth cannot be identified and, therefore, its value is set to zero.

The handling qualities deterioration in right-handed turns is related to specific changes in the pitch frequency response that occur with increasing load factor. Figure 3 integrates three plots. The top two show the on-axis frequency response in pitch for three values of the load factor n_T . The advance ratio is $\mu = 0.1$ and the turns are to the right. A notch is present at about 7 rad/s, which is the frequency of the regressive lag mode. As the load factor increases, both the magnitude and the phase curves show valleys that become deeper and move toward higher frequencies. These valleys result in a premature crossing of the -180 -deg phase delay line for the curves with $n_T = 1.375$ and 1.5 . As a consequence, these two curves have a frequency ω_{180} of only about 1.7–1.8 rad/s instead of about 4.5–5 rad/s for lower load factors. The phase bandwidth is consequently also much lower and is equal to about 1.6 rad/s. Another consequence of the reduced crossover frequencies for $n_T \geq 1.375$ is that the gain bandwidth $\omega_{BW_{gain}}$ becomes extremely low: to obtain a 6-dB gain margin with respect to the gain at the crossover frequency, it is necessary to go well below 0.1 rad/s. The phase delays are very large for both values of n_T ; this is primarily due to the depth of the valleys in the phase curves. For $n_T = 1$ and 1.125 , magnitude and phase curves do not show any noteworthy features from the handling qualities point of view: in both cases level 1 is easily reached. For the intermediate value $n_T = 1.25$, the valley in the phase curve crosses the -135 -deg delay line, but not the -180 -deg line. As a

consequence, the ω_{180} frequency is essentially the same as for the lower load factors, but the phase bandwidth is substantially smaller. The gain bandwidth is also considerably lower. In fact, the magnitude curve has a hump around 3 rad/s that is not sufficient to provide the required 6 dB of gain margin, and it is necessary to go down to just below 2 rad/s. Above 1.5–2 rad/s the phase curve is generally similar to those for the lower load factors and, therefore, the phase delay increases only slightly.

To understand the reasons for the changes in the magnitude and phase curves it is useful to consider how poles and zeros of the helicopter change with load factor. The bottom plot of Fig. 3 shows the change in the undamped natural frequency ω_n of poles and zeros as a function of turn rate. The frequency scale is the same as in the Bode plots in the upper part of the figure. There are four poles in the frequency range of interest, all of which appear as stable complex conjugate pairs. The frequencies of the phugoid and of the short-period poles increase with load factor while that of the Dutch roll decreases slightly; these trends are in qualitative agreement with those reported in Ref. 5. The frequency of the regressive lag pole remains essentially constant. In straight flight this pole is almost exactly canceled by a zero. As the load factor increases, the separation between the pole and the zero increases slightly; because of this, and because both are lightly damped, the size of the peak and the notch in the magnitude and phase plots increase with increasing turn rate. More interesting, from a handling qualities point of view, is the evolution of the other zero plotted in the figure. In straight flight, $n_T = 1$, this zero is close to the Dutch roll pole. Exact cancellation does not occur, indicating that some coupling between longitudinal and lateral dynamics exists for this configuration even in straight flight. As the load factor increases, so does the frequency of this zero and, consequently, the separation from the Dutch roll pole; this is a sign of increased coupling, which is expected to occur in turning flight.⁵ The bottoms of the valleys in the magnitude and phase plots occur at frequencies that are close to that of the zero. Therefore, the migration of this zero helps explain the changes in the shapes of the magnitude and phase curves; these in turn are responsible for the changes in bandwidth and phase delay with load factor discussed earlier. Consequently, the deterioration in longitudinal handling qualities can be seen as an indirect effect of the increased coupling between longitudinal and lateral directional dynamics that occurs in turning flight.

The pitch frequency response and the frequencies of poles and zeros at $\mu = 0.2$ are shown in Fig. 4 for the same values of load factors as in Fig. 3. The bottom plot in the figure shows that the general behavior with frequency of poles and zeros is similar to that at $\mu = 0.1$. The same poles dominate the frequency band from 1 to 10 rad/s, namely: phugoid, Dutch roll, short period, and regressive lag. A complex-conjugate zero is close to the regressive lag pole, and both have very low damping. This results in the valley/peak pattern around 7 rad/s. Another complex-conjugate zero cancels the Dutch roll pole in straight flight and moves to higher frequencies as the turn rate increases. The movement of this relatively lowly damped zero causes valleys in the magnitude and phase plots for all turning flight conditions. These valleys produce a premature crossing of the -135 -deg phase line for all values of $n_T > 1$ shown in Fig. 4. Therefore, the phase bandwidth $\omega_{BW_{phase}}$ drops from 3.5 rad/s for $n_T = 1$ to 2.4 rad/s for $n_T = 1.125$ and decreases further with increasing n_T . As to the -180 -deg phase line, the premature crossings occur for slightly larger values of n_T , that is, for $n_T \geq 1.25$. Therefore, a sharp drop of frequency ω_{180} occurs for those values of n_T ; ω_{180} goes from 5.5 and 4.9 rad/s for $n_T = 1$ and 1.125 , respectively, to 2.9 rad/s for $n_T = 1.25$. This substantial reduction affects the value of the gain bandwidth $\omega_{BW_{gain}}$. In fact, the reduced values of crossover frequencies for $n_T \geq 1.25$ correspond to points on the hump below 2.5–3 rad/s of the magnitude curve; adding the required 6-dB gain margin leads to a gain bandwidth from 1.8 rad/s for $n_T = 1.25$ down to 1.4 rad/s for $n_T = 1.5$. This last value is not entirely correct because the maximum of the magnitude curve falls short by about 0.3 dB of the required 6 dB. The system is phase limited for $n_T = 1$ and 1.125 and gain limited for $n_T \geq 1.25$.

Helicopters can have dynamics in right-handed turns different from that in left-handed turns.^{5,7} Figure 5 shows frequency response

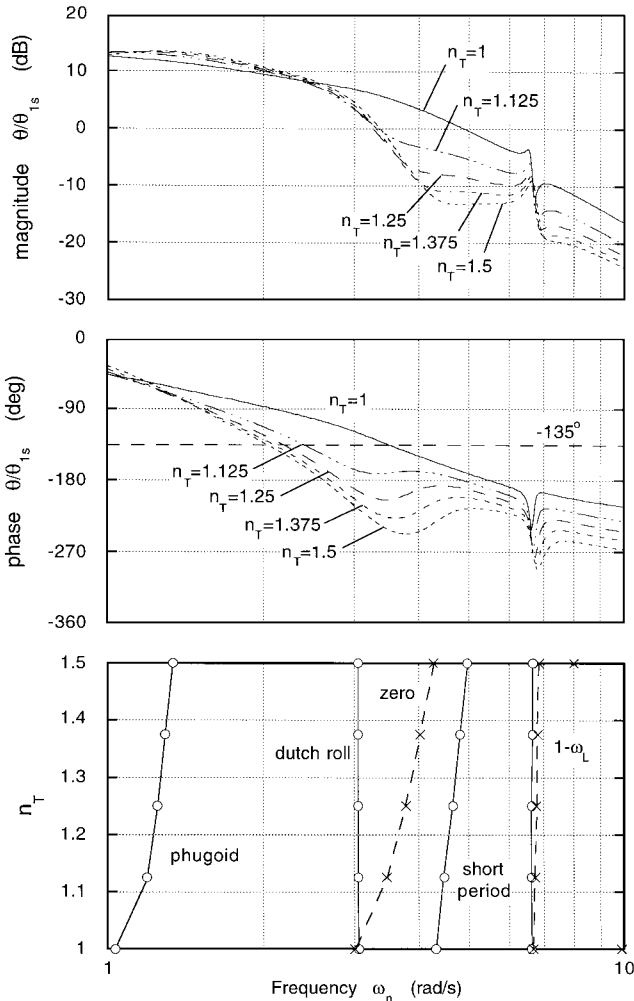


Fig. 4 Effect of load factor n_T on pitch frequency response and on poles and zeros; right-handed turns at $\mu = 0.2$.

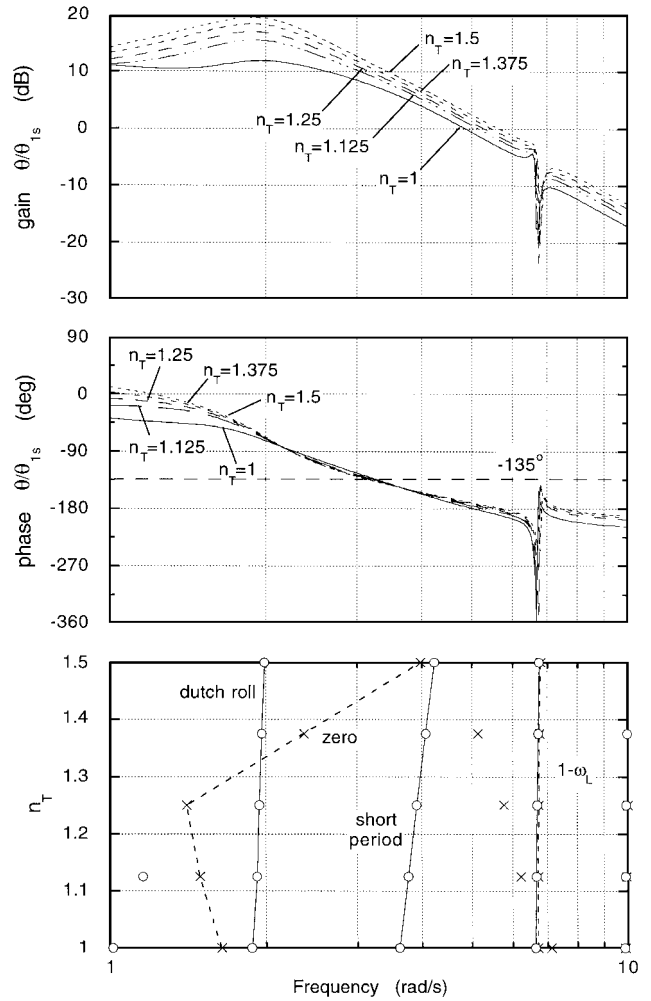


Fig. 5 Effect of load factor n_T on pitch frequency response and on poles and zeros; left-handed turns at $\mu = 0.1$.

and pole/zero curves for the same flight conditions and load factors as Fig. 3, except that the turns are left handed (or counterclockwise when seen from above). It is interesting to note that magnitude and phase curves show none of the valleys observed for right-handed turns. The valley/peak pattern associated with the rotor lag regressive mode remains, but otherwise the frequency response curves show only small and gradual variations with n_T . The magnitudes increase because of the increase in control effectiveness brought about by the increasing load factor. The frequency ω_{180} increases from 5 to 5.7 rad/s as n_T increases from 1 to 1.5. The gain bandwidth $\omega_{BW\text{gain}}$ increases smoothly from 3.7 to 4.3 rad/s. The phase bandwidth $\omega_{BW\text{phase}}$ decreases slightly from 3.3 to 3.2 rad/s, with the result that the system is phase limited for all values of n_T . Overall, the effect of load factor clearly appears to be much more benign and gradual for left than for right turns. The changes in handling qualities characteristics are correspondingly small and gradual, as shown in Fig. 2 (which also includes data for $\mu = 0.2$). Level 1 is achieved for all turn rates. The variations of gain and phase bandwidth as a function of turn rate, advance ratio, and direction of turn are summarized in Fig. 6.

The frequency changes of poles and zeros as a function of n_T , shown in the bottom part of Fig. 5, are not sufficient to explain the differences between right- and left-handed turns, because the migrations of the zero in the 1.5–4 rad/s band are qualitatively similar to those observed in right-handed turns. What are needed to explain the differences are the values of the damping associated with the zero. The concept of damping ratio ζ of a zero will be used here for convenience, although it does not have the same clear physical interpretation as the damping of a pole. The damping ratio of a zero will be calculated in the same way as that of a pole; a value $\zeta < 0$ denotes a nonminimum-phase zero. Figure 7 shows the value of ζ as

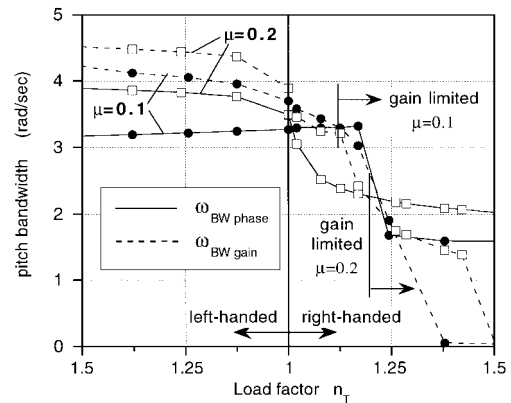


Fig. 6 Effect of load factor n_T on pitch bandwidth.

a function of turn rate for the zero previously identified as responsible for changes in the shapes of the frequency response curves. It is clear from the figure that increasing the turn rate increases the damping for left-handed turns and decreases it for right-handed turns. For an advance ratio $\mu = 0.1$ and load factor $n_T \geq 1.375$, the zero is nonminimum phase; this explains the large phase delays clearly visible in Fig. 3 for those values of n_T . The higher value of ζ in left-handed turns also explains why the zero does not produce the same valleys in the frequency response curves as in the right-handed turns.

It may be interesting to consider the frequency response curves when the output is not the pitch attitude θ but rather the integral of the pitch rate q . This angle, denoted here as θ^* , may give a

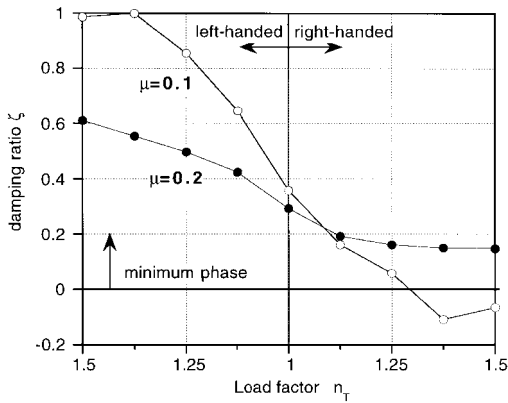


Fig. 7 Effect of load factor n_T on midfrequency pitch zero.

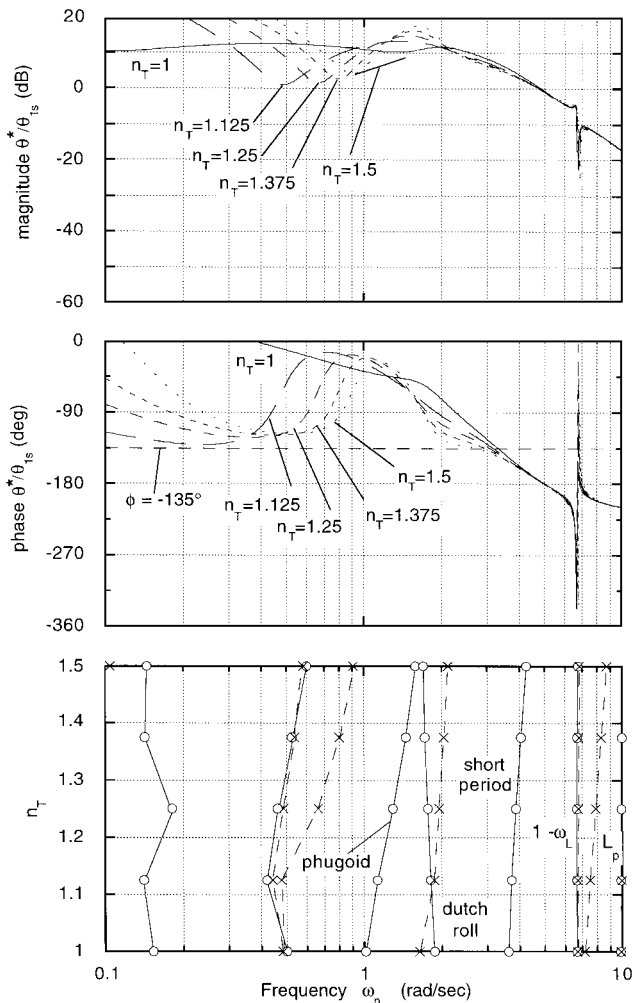


Fig. 8 Effect of load factor n_T on pitch frequency response and on poles and zeros; pitch angle is θ^* , right-handed turns at $\mu = 0.1$.

better indication of attitude changes as seen by the pilot than the angle θ , which is defined with respect to a gravity axis system. The two angles are essentially identical in straight and level flight but become more different as the turn rate increases. Figure 8 shows amplitude, phase, poles, and zeros for right turns at $\mu = 0.1$; it is identical to Fig. 3, except that the output is θ^* instead of θ . In this case, the damping of the midfrequency pitch zero of Fig. 7 still decreases for right-handed turns, but the zero remains minimum phase, and its damping ζ never goes below 0.3. As a result, the changes in the frequency response characteristics are benign, and the handling qualities remain at level 1 at all turn rates. The crossing of the -180 -deg phase line is essentially unaffected by turn rate, as is the gain bandwidth. The phase bandwidth decreases slightly with

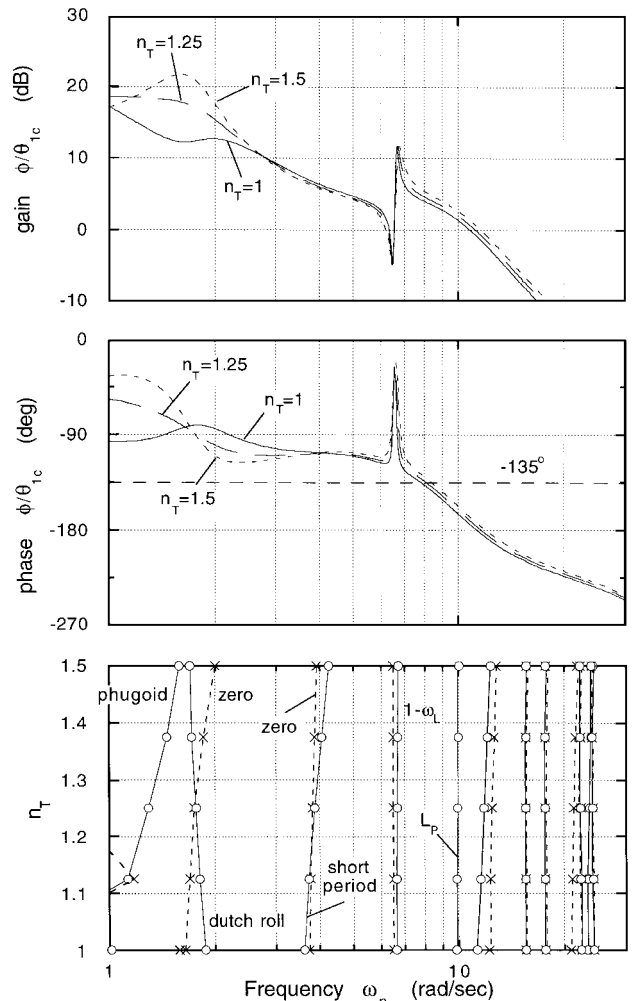


Fig. 9 Effect of load factor n_T on roll frequency response and on poles and zeros; right-handed turns at $\mu = 0.1$.

turn rate; the valleys in the phase curves are very close at the -135 -deg phase line at low frequency but do not cross it.

Roll Dynamics

The on-axis frequency response in roll is shown in Fig. 9 from 1 to 30 rad/s, for different values of the load factor and $\mu = 0.1$; all of the turns are to the right. The undamped natural frequencies of poles and zeros are also shown in Fig. 9 as a function of load factor. Two complex poles and one complex zero appear in the 1–2 rad/s band. The lower frequency pole corresponds to the phugoid; for $n_T \leq 1.125$ this pole is essentially canceled by a zero, the behavior of which is partially shown in Fig. 9. At higher load factors this zero disappears from the frequency band shown, and the coupling increases. The second pole pair corresponds to the Dutch roll mode. The zero remains in the vicinity of this mode, and its frequency increases slightly with load factor. Other noteworthy features shown in Fig. 9 are the short-period (pitch) pole pair around 4 rad/s, which is nearly canceled by a complex zero for all load factors, and the notch/peak pattern around 7 rad/s corresponding to the lag regressive pole pair that is nearly canceled by a zero pair, both pairs lightly damped. The pole at about 10 rad/s corresponds to the roll or L_p mode.

The behavior of the zero near the Dutch roll pole has some similarities with that of the pitch zero discussed earlier, but its effects on the roll frequency response are quite different. In fact, it does not trigger any major changes in the shape of the magnitude or the phase curves. Phase bandwidth and crossover frequency exhibit small and smooth changes with load factor, and the same is true for the gain bandwidth if the response peak around 7 rad/s is ignored when locating the point with 6-dB gain margin. The zero remains minimum phase for all of the turning flight conditions and is well damped except for left turns at $\mu = 0.1$; this helps explain

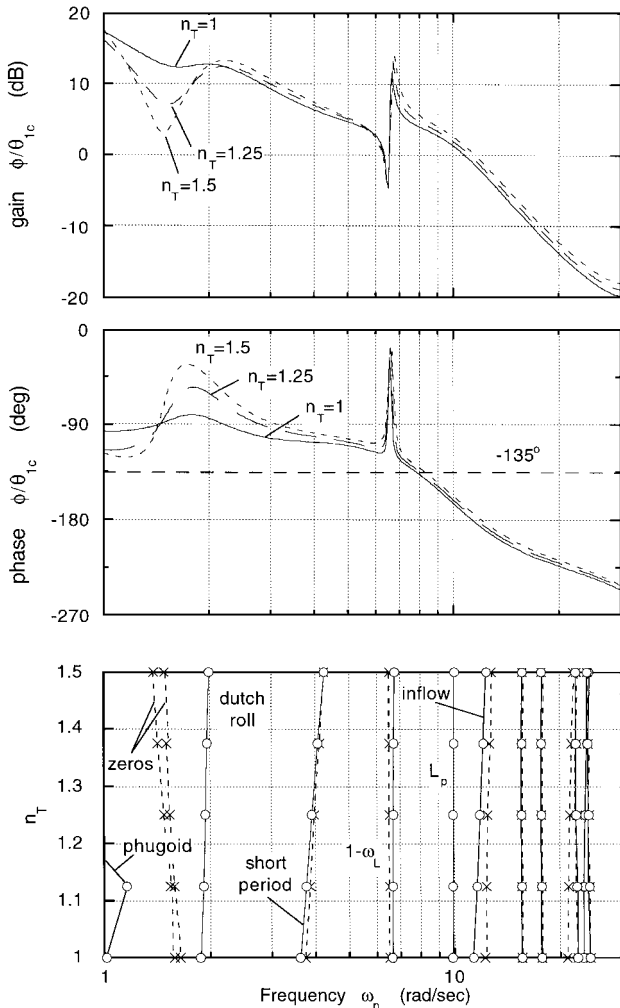


Fig. 10 Effect of load factor n_T on roll frequency response; left-handed turns at $\mu = 0.1$.

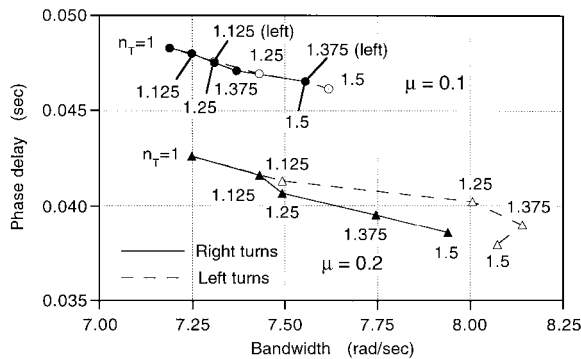


Fig. 11 Effect of load factor n_T and direction of turn on roll bandwidth and phase delay.

the differences between pitch and roll frequency responses for the same flight conditions (Figs. 3 and 9). For left turns at $\mu = 0.1$, the damping is lowest, with $\zeta = 0.09$. Figure 10 shows the frequency response for $n_T = 1, 1.25, \text{ and } 1.5$. The zero and the Dutch roll pole interact below 2 rad/s, with noticeable decreases in magnitude and increases in phase delay for increasing n_T . However, the differences in gain above 2 rad/s are modest, and phase bandwidth and crossover frequency increase only slightly with load factor.

Figure 11 shows bandwidth and phase delay as functions of load factor and direction of turn for $\mu = 0.1$ and 0.2. The quantities are calculated following the criteria of ADS-33D.¹ In all cases the points are well within the region of level 1 handling qualities. However, it should be kept in mind that the phase delays shown in Fig. 11 (and those shown in Fig. 2 for pitch) are optimistic because they only include the effect of fuselage and rotor dynamics. Other important

sources of delays, such as swashplate actuators, sensor and computation delays have not been modeled in this study. In all cases the bandwidth corresponds to the phase bandwidth, i.e., the system is phase limited. The results show that the bandwidth tends to increase with turn rate; this is likely due to the increase of roll damping L_p in turns (increase also observed in Refs. 5 and 6). In fact, it can be shown that for a first-order approximation to the $\phi(s)/\theta_{1c}(s)$ transfer function and for $n_T = 1$ the phase bandwidth is equal to $-L_p$. The phase delay also tends to decrease with load factor.

Heave Dynamics

The top portion of Fig. 12 shows the heave frequency response to collective pitch for right-handed turns at an advance ratio $\mu = 0.1$, for frequencies between 0.5 and 30 rad/s; the bottom portion shows the undamped natural frequencies of poles and zeros as a function of load factor for the same frequency band. The main feature of the magnitude plot is a valley below 3 rad/s, of depth varying from about 10 dB in straight flight to more than 20 dB for $n_T = 1.5$. The frequency at which the bottom of the valley occurs decreases with increasing load factor. This is due to the interaction of two pairs of complex conjugates, lowly damped poles (phugoid and Dutch roll), one real zero, and two complex-conjugate pairs of zeros. There are essentially no cancellations among these poles and zeros, with the short-period pole around 4 rad/s; therefore, the dynamics stays coupled at all load factors. At the highest load factor $n_T = 1.5$, there is a substantial increase in phase delay at about 1.3 rad/s. The damping ratio of the three zeros in the 1–3 rad/s band is shown in Fig. 13. The lowest frequency zeros also have the lowest damping, which decreases with turn rate and becomes slightly negative at $n_T = 1.5$. Therefore, the increased phase delay observed in Fig. 12 for $n_T = 1.5$ is due to this nonminimum-phase zero. Finally, Fig. 14 shows the

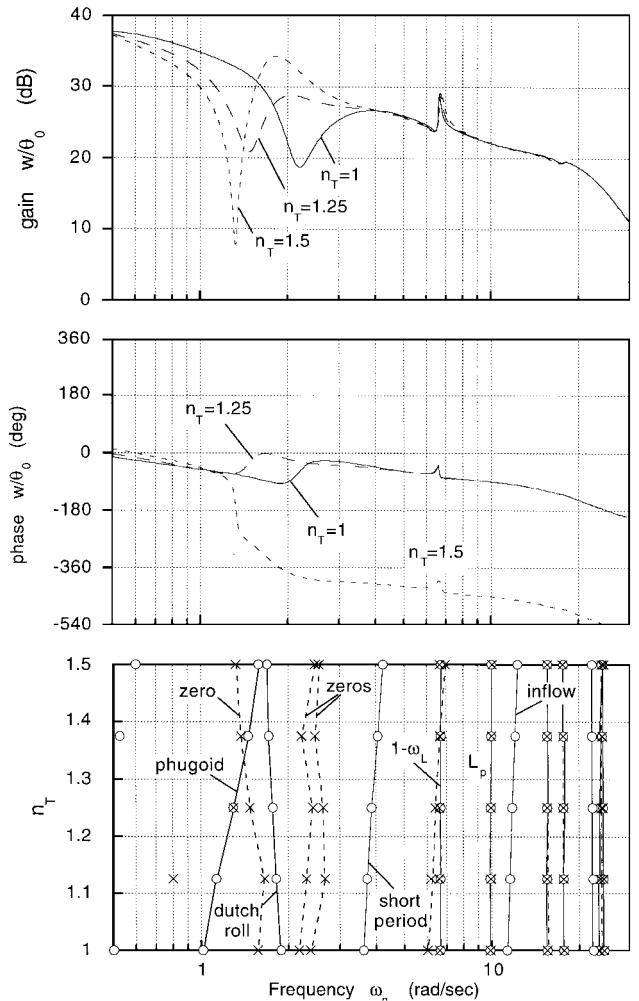


Fig. 12 Effect of load factor n_T on heave frequency response and on poles and zeros; right-handed turns at $\mu = 0.1$.

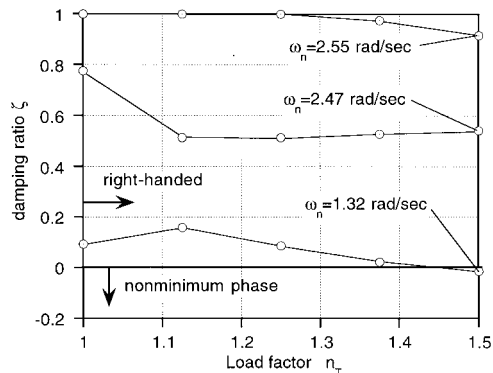


Fig. 13 Effect of load factor n_T on heave zeros; right-handed turns at $\mu = 0.1$.

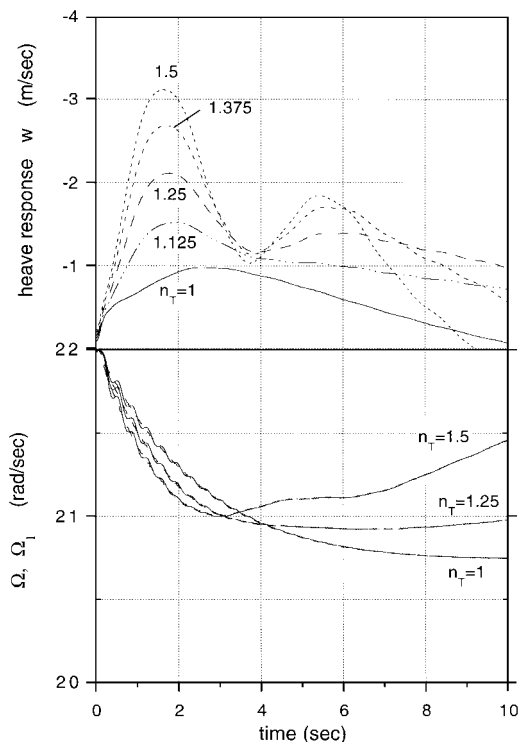


Fig. 14 Heave and revolutions per minute response to 1 deg of collective pitch; right-handed turns at $\mu = 0.1$.

time history of the response of heave and propulsion system speeds to a one-degree step input of collective pitch. The angular velocities of the rotor, Ω , and of the transmission at the exit of the gearbox, Ω_1 , are essentially superimposed in the scale of Fig. 14 (although the effects of propulsion system dynamics are clearly visible in enlarged views). The heave velocity response becomes more and more oscillatory as n_T increases because of the reduction in damping of the zero already mentioned. The frequency is that of the phugoid mode, which for these flight conditions is also close to that of the Dutch roll.

For n_T , Fig. 14 does not show the inversion of the initial slope of the heave response w that would be expected in the presence of a nonminimum-phase zero. The reason is the zeros are calculated from the linearized model of the helicopter, whereas the time histories are calculated from the full nonlinear model. For small-amplitude inputs the differences are small, but in this case they are sufficient to produce minimum-phase-type responses with a zero only slightly in the right-half plane. The response calculated from the linearized model, not shown here, does, indeed, show an inversion of the slope of the initial response.

Additional Comments

Comparing the effects of zeros for the various axes, it is possible to conclude that the changes in frequency and damping of a zero with load factor can explain large changes in the shapes of the frequency

response curves. These changes can then translate into degradations in handling qualities in turning flight. However, the presence of one or more lowly damped zeros does not necessarily affect handling qualities. Whether or not it does also depends on the frequency of the zeros and on their separation from nearby poles (which may be canceled, or near canceled, in straight flight). Note that the helicopter remains stable for all of the flight conditions considered in this study, and, therefore, any possible degradation of handling qualities should not be attributed to any bare airframe instability.

The results of this study may have practical implications on the design of flight control systems. Reference 5 includes a numerical study of the characteristics of a SCAS designed based on steady straight flight conditions. This SCAS could stabilize the helicopter in left turns at load factors of 1.5 and 2, but not in right turns at the same load factors. In light of the results of the present study, it is possible that the degradation in right turns may have been caused by the presence of a nonminimum-phase zero that was stable in straight flight and that attracted the closed-loop system poles into an unstable region. Lowly damped or nonminimum-phase zeros may also appear in the heave response. Therefore, if the helicopter is equipped with a governor to keep the rotor speed constant, and if the governor has been designed based on straight flight conditions, it is prudent to verify the design in turning flight to guard against possible degradations in performance induced by these zeros.

The results presented indicate that one of the effects of the migration of the zero is to make the aircraft gain limited in some turning flight conditions. In ADS-33 the inclusion of the gain bandwidth in the requirements is intended to avoid flat portions of the magnitude curves. These are associated with rapid reductions of phase margin for small changes in pilot gain and may result in a pilot-induced-oscillation-prone aircraft.¹¹ In the present study, however, a direct application of ADS-33 criteria results in gain-limited configurations that do not exhibit these precise characteristics. Therefore, there remains an open question of whether the low, gain-limited bandwidth in turning flight is a sort of mathematical artifact or whether it does correspond to a real degradation of handling qualities, possibly through mechanisms other than those intended in the original formulation of the ADS-33 specification. For example, if the ADS-33 criteria are applied with a pseudo-pitch angle θ^* given by the integral of the pitch rate q , rather than with the true pitch angle θ , no substantial deterioration in handling qualities is predicted.

If these degradations are real, this would also have implications in pilot-in-the-loop, real-time flight simulations. Handling qualities studies such as those of Refs. 12 and 13 are an example: their purpose was to determine through piloted simulations the magnitudes of pitch and roll bandwidth, normal load factors, and other parameters required to achieve level 1 handling qualities in air-to-air combat missions. Substantial portions of the simulation were conducted in turning flight. The mathematical model driving the simulation included the effect of load factor on pitch and roll rate damping derivatives and neglected control or response couplings.¹⁴ Because the handling qualities degradations identified in the present study are ultimately traced to longitudinal/lateral directional coupling effects, including these effects in mathematical models that drive real-time simulations could improve the fidelity of the simulations and the accuracy of the conclusions drawn from them.

Summary and Conclusions

Results were presented of a theoretical study of some aspects of the flight dynamics of hingeless single-rotor helicopters in turning flight conditions. Frequency response characteristics in pitch and roll were evaluated for various advance ratios, turn rates, and turn directions and were compared with the criteria of the ADS-33 handling qualities specifications for short-term response to pilot inputs. Frequency responses in heave were also presented and discussed. A representative (but hypothetical) helicopter configuration was used.

The main conclusions of the present study are as follows:

- 1) Couplings between lateral and longitudinal dynamics are present in turning flight. The separation of at least one pole-zero pair, at frequencies below 3–4 rad/s, increases with load factor. Flight speed, load factor, and direction of turn affect frequency and damping of both poles and zeros.

2) In some turning flight conditions, zeros that are stable in straight flight can become lowly damped and then unstable, or nonminimum phase. In the present study, this occurred in the pitch degree of freedom for one complex zero at an advance ratio $\mu = 0.1$ and right-handed turns. The migration of the zero changed the shape of the frequency response curves and caused a deterioration of handling qualities according to the ADS-33 criteria. A lowly damped zero that became nonminimum phase at a load factor of 1.5 was also observed in the heave frequency response.

3) The presence of one or more lowly damped zeros does not necessarily affect handling qualities. Whether or not it does also depends on the frequency of the zeros and on their separation from nearby poles. Because the helicopter was stable in all flight conditions, possible degradations of handling qualities should not be attributed to bare airframe instabilities.

4) Changes in frequency and damping of the zeros, and in particular the appearance of nonminimum-phase zeros, may cause flight control systems designed for straight flight to perform poorly in some turning flight conditions.

5) The bandwidth criteria of ADS-33 do not explicitly address maneuvering flight conditions. Therefore, there remains an open question of whether the degradations of handling qualities identified in this study are real (possibly through mechanisms other than those intended in the original formulation of the specification) or some sort of mathematical artifact. For example, the deteriorations in pitch handling qualities all but disappear if the criteria are applied with a pseudopitch angle θ^* given by the integral of the pitch rate q , rather than with the true pitch angle θ .

Acknowledgment

The authors wish to thank Mark Tischler, U.S. Army, for pointing out the potential role of the pseudopitch angle θ^* in the questions-and-answers period following the presentation of the conference version of this paper.

References

¹"Aeronautical Design Standard ADS-33D, Handling Qualities Requirements for Military Rotorcraft," U.S. Army Aviation and Troop Command,

St. Louis, MO, July 1994.

²Padfield, G. D., *Helicopter Flight Dynamics: The Theory and Application of Flying Qualities and Simulation Modeling*, AIAA Education Series, Washington, DC, 1995, Chaps. 6, 7.

³Chen, R. T. N., and Jeske, J. A., "Kinematic Properties of the Helicopter in Coordinated Turns," NASA TP 1773, April 1981.

⁴Chen, R. T. N., Jeske, J. A., and Steinberger, R. H., "Influence of Sideslip on the Flight Dynamics of Rotorcraft in Steep Turns at Low Speeds," 39th Annual Forum of the American Helicopter Society, St. Louis, MO, 1983.

⁵Chen, R. T. N., "Flight Dynamics of Rotorcraft in Steep High-g Turns," *Journal of Aircraft*, Vol. 21, No. 1, 1984, pp. 14-22.

⁶Houston, S. S., "On the Analysis of Helicopter Flight Dynamics During Manoeuvres," Eleventh European Rotorcraft Forum, Paper No. 80, London, 1985.

⁷Celi, R., "Hingeless Rotor Dynamics in Coordinated Turns," *Journal of the American Helicopter Society*, Vol. 36, No. 4, 1991, pp. 39-47.

⁸Spence, A. M., and Celi, R., "Coupled Rotor-Fuselage Dynamics and Aeroelasticity in Turning Flight," *Journal of the American Helicopter Society*, Vol. 40, No. 1, 1995, pp. 47-58.

⁹Peters, D. A., and HaQuang, N., "Dynamic Inflow for Practical Applications," *Journal of the American Helicopter Society*, Vol. 33, No. 4, 1988, pp. 64-68.

¹⁰Chen, R. T. N., "An Exploratory Investigation of the Flight Dynamic Effects of Rotor RPM Variations and Rotor State Feedback in Hover," Eighteenth European Rotorcraft Forum, Paper No. 20, Avignon, France, 1992.

¹¹Hoh, R. H., "Dynamic Requirements in the New Handling Qualities Specification for U.S. Military Rotorcraft," Royal Aeronautical Society International Conf. on Helicopter Handling Qualities and Flight Control, London, 1988, pp. 4.1-4.18.

¹²Whalley, M. S., and Carpenter, W. R., "A Piloted Simulation Investigation of Pitch and Roll Handling Qualities Requirements for Air-to-Air Combat," 48th Annual Forum of the American Helicopter Society, Washington, DC, 1992, pp. 723-735.

¹³Whalley, M. S., "A Piloted Simulation Investigation of the Normal Load Factor and Longitudinal Thrust Required for Air-to-Air Acquisition and Tracking," NASA Ames/AHS Conf. on Piloting Vertical Flight Aircraft, San Francisco, CA, 1993, pp. 2-1-2-18.

¹⁴Whalley, M. S., "Development and Evaluation of an Inverse Solution Technique for Studying Helicopter Maneuverability and Agility," NASA TM-102889 and USAAVSCOM TR 90-A-008, July 1991.